

Diffusion and ballistic contributions of the interaction correction to the conductivity of a two-dimensional electron gas

G. M. Minkov and A. A. Sherstobitov
Institute of Metal Physics RAS, 620219 Ekaterinburg, Russia

A. V. Germanenko, O. E. Rut, and V. A. Larionova
Institute of Physics and Applied Mathematics, Ural State University, 620083 Ekaterinburg, Russia

A. K. Bakarov
Institute of Semiconductor Physics, 630090 Novosibirsk, Russia

B. N. Zvonkov
Physical-Technical Research Institute, University of Nizhni Novgorod, 603600 Nizhni Novgorod, Russia
 (Dated: November 21, 2018)

The results of an experimental study of interaction quantum correction to the conductivity of two-dimensional electron gas in A_3B_5 semiconductor quantum well heterostructures are presented for a wide range of $T\tau$ -parameter ($T\tau \simeq 0.03 - 0.8$), where τ is the transport relaxation time. A comprehensive analysis of the magnetic field and temperature dependences of the resistivity and the conductivity tensor components allows us to separate the ballistic and diffusion parts of the correction. It is shown that the ballistic part renormalizes in the main the electron mobility, whereas the diffusion part contributes to the diagonal and does not to the off-diagonal component of the conductivity tensor. We have experimentally found the values of the Fermi-liquid parameters describing the electron-electron contribution to the transport coefficients, which are found in a good agreement with the theoretical results.

PACS numbers: 73.20.Fz, 73.61.Ey

I. INTRODUCTION

The temperature and magnetic field dependences of the resistivity of the degenerated two dimensional (2D) gas at low temperatures are determined by the quantum corrections to the conductivity. They are the weak localization (WL) or interference correction and the correction caused by the electron-electron ($e-e$) interaction. The WL correction to the conductivity in the absence of the spin relaxation is negative and logarithmically increases in absolute value with decreasing temperature. The interaction correction for low r_s -values and within the diffusion regime, $T\tau \ll 1$ (where r_s is the gas parameter, and τ is the transport relaxation time, hereafter we set $\hbar = 1$, $k_B = 1$) is, as a rule, negative and also increases in absolute value with the temperature decrease. However, the detailed theoretical analysis of the interaction correction to the conductivity for the intermediate ($T\tau \simeq 1$) and ballistic ($T\tau \gg 1$) regimes carried out in Refs. 1,2,3 shows that this correction can result in different sign of the T -dependence of the resistivity. It is dictated by the value of the Fermi-liquid constant (see Figs. 7 and 8 in Ref. 1). Just this fact comes to special attention to the interaction correction in ballistic regime because it can explain the metallic-like temperature dependence of the conductivity^{4,5,6,7} observed in some 2D structures.

The $e-e$ correction in the diffusion regime can be easily separated experimentally because it contributes only to diagonal components of the conductivity tensor and

does not to off-diagonal one. It is more difficult to extract experimentally the correction in the intermediate and the ballistic regimes because the theories does not divide the interaction correction into the diffusion and ballistic parts and does not predict any specific features of this correction. Besides, some classical mechanisms such as temperature dependent disorder,⁸ classical magnetoresistance due to scattering by rigid scatterers⁹ can complicate the situation.^{5,7} In the ballistic regime, $T\tau \gg 1$, for the white noise disorder and classically low magnetic field, $\mu B \ll 1$, where μ is the mobility, the theory^{1,10} predicts that the $e-e$ interaction contributes both to σ_{xx} and σ_{xy} in such a way that it does not influence the Hall coefficient, R_H . This means that the $e-e$ interaction in this regime reduces to a renormalization of the transport relaxation time. The same result was obtained for the long-range and mixed disorder at high magnetic field, $\mu B \gg 1$, in Refs. 2 and 3.

In this paper we systematically study the $e-e$ interaction correction to the conductivity of n -type $Al_xGa_{1-x}As/GaAs/Al_xGa_{1-x}As$ and $GaAs/In_xGa_{1-x}As/GaAs$ quantum wells. The comprehensive analysis of the data within wide $T\tau$ range ($T\tau = 0.03 - 0.8$) and classically strong magnetic field shows that the interaction correction to the conductivity can be divided into two parts. The first part contributes to σ_{xx} only, it is proportional to $\ln[1/(T\tau) + 1]$ within whole $T\tau$ range (we refer to this part as “diffusion part”), while the second one reduces to renormalization of the transport relaxation time and is proportional to

$T\tau$ (this part is termed as the ‘‘ballistic part’’).

II. THEORETICAL BACKGROUND

The conductivity of a system at zero magnetic field is given by

$$\sigma = \sigma_0 + \delta\sigma^{ee} + \delta\sigma^{WL}. \quad (1)$$

Here, $\sigma_0 = en\mu$ with n as the electron density, is the Drude conductivity, σ^{WL} and $\delta\sigma^{ee}$ stand for the weak-localization and interaction quantum correction, respectively. The weak-localization correction looks as follows

$$\begin{aligned} \frac{\delta\sigma^{WL}}{G_0} &= -\ln\left(1 + \frac{\tau_\phi}{\tau}\right) \\ &+ \frac{1}{1 + 2\tau_\phi/\tau} \ln\left(1 + \frac{\tau_\phi}{\tau}\right) + \frac{\ln 2}{1 + \tau/2\tau_\phi}, \end{aligned} \quad (2)$$

where $G_0 = e^2/(2\pi^2\hbar) \simeq 1.23 \times 10^{-5} \Omega^{-1}$, τ_ϕ is the phase relaxation time, and the second and third terms take into account non-backscattering processes.¹¹ The interaction correction was calculated in Refs. 1 and 3, and for a white noise disorder and wide range of $T\tau$ -values is given by:

$$\begin{aligned} \frac{\delta\sigma^{ee}}{G_0} &= 2\pi T\tau \left[1 - \frac{3}{8}f(T\tau) + \frac{3\tilde{F}_0^\sigma}{1 + \tilde{F}_0^\sigma} \right. \\ &\times \left. \left(1 - \frac{3}{8}t(T\tau, \tilde{F}_0^\sigma) \right) \right] \\ &- \left[1 + 3 \left(1 - \frac{\ln(1 + F_0^\sigma)}{F_0^\sigma} \right) \right] \ln \frac{E_F}{T}, \end{aligned} \quad (3)$$

The functions $f(T\tau)$ and $t(T\tau, \tilde{F}_0^\sigma)$ are given in Ref. 1. In contrast to Eq. (2.16c) of this paper we have explicitly written the different Fermi-liquid constants in the first and second terms of Eq. (3) (see last paragraph in pages 5 of the same paper). When the $T\tau$ -value is low enough, the temperature dependence of $\delta\sigma^{ee}$ is controlled by the second term in Eq. (3) and it is logarithmic. For the high $T\tau$ -value, the first term in Eq. (3) becomes dominant, because the functions $f(T\tau)$ and $t(T\tau, \tilde{F}_0^\sigma)$ go to zero when $T\tau \rightarrow \infty$. In this limit, the conductivity changes with the temperature linearly. Noteworthy is the argument of the logarithm in Eq. (3), which is written by the authors as E_F/T instead of the usual $1/T\tau$.¹²

Unfortunately, it is not sufficient for the reliable determination of $\delta\sigma^{ee}$ to know the behavior of the interaction correction in the absence of magnetic field. The reason is the other temperature dependent scattering mechanisms, for instance, phonon scattering or the temperature-dependent disorder,⁸ which can be presented in real systems and can mask the effect under consideration. Investigations in the presence of magnetic field are much more informative from this point of view.

In a magnetic field the conductivity tensor can be written as

$$\sigma_{xx} = \frac{en\mu}{1 + \mu^2 B^2} + \delta\sigma_{xx}^d + \delta\sigma_{xx}^b, \quad (4)$$

$$\sigma_{xy} = \frac{en\mu^2 B}{1 + \mu^2 B^2} + \delta\sigma_{xy}^b, \quad (5)$$

where $\delta\sigma_{xx}^d$ and $\delta\sigma_{xx}^b$ are the diffusion and ballistic parts of the interaction correction. It is important to mention here that the diffusion part of the electron-electron interaction contributes to σ_{xx} only and does not to σ_{xy} .¹² This is a key feature of the diffusion correction, which allows one to determine its value experimentally. The diffusion correction $\delta\sigma_{xx}^d$ logarithmically depends on the temperature and does not depend on the magnetic field (the latter is true if the Zeeman splitting is less than T). It is usually written as^{12,13,14}

$$\begin{aligned} \frac{\delta\sigma_{xx}^d(T)}{G_0} &= - \left[1 + 3 \left(1 - \frac{\ln(1 + F_0^\sigma)}{F_0^\sigma} \right) \right] \ln \frac{1}{T\tau} \\ &\equiv K_{ee} \ln T\tau, \end{aligned} \quad (6)$$

where the first term in square brackets is the exchange or the Fock contribution while the second one is the Hartree contribution (the triplet channel). Comparing Eq. (3) with Eq. (6) one can see that the arguments in logarithms in these expressions are different and distinguished by a factor $E_F\tau = k_F l/2$. Thus, the question whether the argument in the logarithm in Eq. (6) is E_F/T or $1/(T\tau)$ is open.

As for the ballistic contributions, the situation is more complicated. The ballistics contribute both to σ_{xx} and to σ_{xy} , and, in general case, $\delta\sigma_{xx}^b$ and $\delta\sigma_{xy}^b$ depend both on the magnetic field and temperature. For the low magnetic field, $B \ll 1/\mu$, and white-noise disorder the corrections to the conductivity tensor components were calculated in Refs. 1,10, while for the high magnetic field and smooth or mixed disorder it was done in Ref. 3. The results for all the cases are different, however, the analysis shows that in the limiting case $T\tau \gg 1$ the interaction correction universally reduces to a renormalization of the transport relaxation time. It is physically understandable because the interaction correction in this regime can be considered as a result of elastic scattering of an electron by the temperature-dependent self-consistent potential created by all the other electrons.¹ It is reasonable to generalize this result and to assume that the ballistic correction reduces in the most part to the renormalization of the transport relaxation time, i.e., to the renormalization of the mobility for any values of $T\tau$ -parameter. Then, Eqs. (4) and (5) can be rewritten as follows

$$\sigma_{xx} \simeq \frac{en\mu'}{1 + \mu'^2 B^2} + \delta\sigma_{xx}^d, \quad (7)$$

$$\sigma_{xy} \simeq \frac{en\mu'^2 B}{1 + \mu'^2 B^2}, \quad (8)$$

where $\mu' = \mu + \delta\mu$ is the mobility renormalized by the ballistics. Such an assumption is in accordance with the results for different limiting cases obtained the papers cited above. In particular, within these frameworks one obtains the logarithmic behavior of $\sigma(B = 0)$, σ_{xx} and the Hall coefficient at low temperatures, $T \ll 1/\tau$, and

the vanishing of the interaction correction to the Hall coefficient at $T\tau \rightarrow \infty$.^{1,3}

In what follows we will show that such a model for the ballistic correction well describes the experimental data at low and intermediate temperatures up to $T\tau \simeq 1$.

Below we will name that part of the interaction correction which contributes to $\sigma_{xx}(B)$ but does not to $\sigma_{xy}(B)$ as “the diffusion correction” because just the same property has the $e-e$ correction in the diffusive regime. The part of interaction correction which renormalizes the mobility $en\delta\mu$ we will name as “the ballistic correction”.

III. EXPERIMENT

We study the interaction correction to the conductivity in heterostructures of two types. The first one is the $\text{Al}_x\text{Ga}_{1-x}\text{As}/\text{GaAs}/\text{Al}_x\text{Ga}_{1-x}\text{As}$ quantum well heterostructure grown by MBE on semiinsulator GaAs substrate. It consists of 250 nm-thick undoped GaAs buffer layer, a 50 nm $\text{Al}_{0.3}\text{Ga}_{0.7}\text{As}$ barrier, Si δ -layer, a 6 nm spacer of undoped $\text{Al}_{0.3}\text{Ga}_{0.7}\text{As}$, a 8 nm GaAs well, a 6 nm spacer of undoped $\text{Al}_{0.3}\text{Ga}_{0.7}\text{As}$, a Si δ -layer, a 50 nm $\text{Al}_{0.3}\text{Ga}_{0.7}\text{As}$ barrier, and 200 nm cap layer of undoped GaAs. The second structure is $\text{GaAs}/\text{In}_x\text{Ga}_{1-x}\text{As}/\text{GaAs}$ structure. It consists of a 200 nm-thick undoped GaAs buffer layer, Si δ -layer, a 9 nm spacer of undoped GaAs, a 8 nm $\text{In}_{0.2}\text{Ga}_{0.8}\text{As}$ well, a 9 nm spacer of undoped GaAs, a Si δ -layer, and 200 nm cap layer of undoped GaAs. The samples were mesa etched into standard Hall bars and then an Al gate electrode was deposited by thermal evaporation onto the cap layer of the first structure through a mask. Varying the gate voltage V_g from 1 V to -4 V we decreased the electron density in the quantum well from $1.7 \times 10^{12} \text{ cm}^{-2}$ to $7 \times 10^{11} \text{ cm}^{-2}$. The electron density in the second structure was controlled through the illumination due to the persistent photoconductivity effect. The measurements were performed after the illumination of the different intensity and duration that allowed us to change the electron density within the range from $4.3 \times 10^{11} \text{ cm}^{-2}$ to $7 \times 10^{11} \text{ cm}^{-2}$. Analysis of the Shubnikov-de Haas oscillations in the first structure shows that the second subband starts to be occupied at $V_g \simeq 0$. In order to prevent the multiband effects we will analyze the results obtained for $V_g \leq -1$ V, when the excited subbands lay far above the Fermi level and are practically empty for the actual temperature range. (So for $V_g = -1$ V, the Fermi level lies about 5 meV below the bottom of the second subband and the estimated value of the electron density in this subband is about 10^8 cm^{-2} for $T = 10$ K. For the lower temperatures and gate voltages this quantity is far less).

We measured carefully the low and high magnetic field longitudinal (ρ_{xx}) and transverse (ρ_{xy}) magnetoresistance in a magnetic field up to 5 T within the temperature range from 0.4 to 25 K. The detailed measurements were performed for three gate voltages for the first struc-

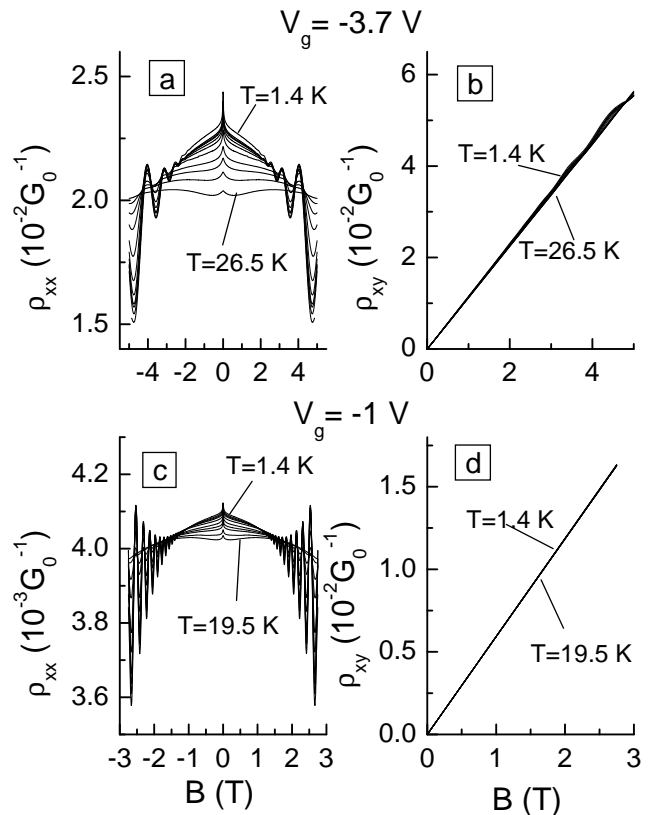


FIG. 1: The magnetic field dependences of ρ_{xx} (a,c) and ρ_{xy} (b,d) measured for different temperatures and $V_g = -3.7$ V (a,b) and -1 V (c,d). Structure T1520. The temperature for curves are: 1.4, 2.0, 2.5, 3.0, 4.2, 6.2, 9.0, 13.0, 16.5, 20.0, 26.5 K (a,b) and 1.4, 2.0, 2.5, 3.0, 4.2, 6.0, 8.5, 11.0, 16.0, 19.5 K (c,d).

ture and after three illumination flux for the second one. The main parameters of the structures are given in Table I, in which B_{tr} stands for the transport magnetic field defined as $B_{tr} = \hbar/2el^2$, where l is the mean free path. The electron density and mobility have been found from the fit of σ_{xy} -vs- B plots, the value of μ given in the table relates to $T = 0$ and is obtained by a linear extrapolation of the experimental dependence $\mu(T)$ (see text below).

To elucidate the role of the ballistic contribution of the

TABLE I: The parameters of structures investigated

Structure	V_g (V)	n (10^{12} cm^{-2})	μ ($\text{cm}^2/\text{V s}$)	B_{tr} (mT)
T1520	-1.0	1.303	14470	4.4
	-2.5	0.967	8950	15.7
	-3.7	0.715	4925	70.0
3510 ^a		0.44	19300	25.9
		0.56	16000	8.5
		0.7	10400	4.7

^aThe electron density in this structure is changed via the illumination.

e - e interaction we will consider in parallel the experimental data obtained for the structure T1520 for two limiting gate voltages: $V_g = -3.7$ V, when the diffusion contribution is dominant, and $V_g = -1$ V, when the ballistics become important.

Fig. 1 shows the magnetic field dependences of ρ_{xx} and ρ_{xy} measured at different temperatures. One can see from Figs. 1(a) and 1(c) that following the sharp magnetoresistance in low magnetic field [evident at $B \lesssim 0.05$ T in Fig. 1(a) and at $B \lesssim 0.02$ T in Fig. 1(c)], which results from the suppression of the interference quantum correction,¹⁵ the parabolic-like negative magnetoresistance against the background of the Shubnikov-de Haas oscillations is observed. The parabolic-like behavior of ρ_{xx} weakens with the increasing temperature transforming to nonmonotonic one at $T \gtrsim 20$ K. The transverse magnetoresistance ρ_{xy} slightly decreases with increasing temperature [Figs. 1(b) and 1(d)]. On the first sight the behavior of the resistivity tensor components is identical for both gate voltages. However, some quantitative difference occurs as we will show below.

Let us begin our analysis with the temperature dependence of the Hall coefficient, $R_H = \rho_{xy}/B$. Its value has been found from a linear interpolation of the ρ_{xy} -vs- B dependence made in the magnetic field range $-1/\mu \dots 1/\mu$.²⁴ The results are presented as $1/(eR_H)$ -vs- T plots in Figs. 2(a) and 2(b) by the solid symbols. One can see that the quantity $1/(eR_H)$ increases logarithmically with the increasing temperature, while the temperature remains less than 8–10 K. Namely such a behavior is predicted by the theories for the diffusion regime (see Section II). However, at higher temperature the value of $1/(eR_H)$ surprisingly starts to fall.

To understand, whether the high-temperature behavior of $1/(eR_H)$ results from the lowering of the electron density with T -increase or it is a peculiarity of the e - e interaction, the Shubnikov-de Haas oscillations have been analyzed. It turns unfortunately out that it is impossible to find the electron density from the period of the oscillations at high temperature with the accuracy required (as seen from Figs. 2(a) and 2(b) the fall does not exceed 1–2 % in magnitude in our temperature range).

Another way to find the electron density is the analysis of the magnetic field dependence of σ_{xy} because it is unaffected by the e - e interaction in the diffusion regime. The fit of the experimental data by Eq. (8) with n and μ' as the fitting parameters gives a very reproducible result. Fig. 3 shows the result of such a fit made for magnetic field range from $20 B_{tr}$ to $B = 1.5/\mu$. A nice coincidence with the experimental σ_{xy} -plots is evident. The value of n obtained for different temperatures by this way is presented in Figs. 2(a) and 2(b) by open symbols. As seen it is constant at low temperature and decreases at $T > 10$ K, coinciding practically with $1/(eR_H)$ -value at $T \gtrsim 15$ K. Note, such a behavior of $1/(eR_H)$ and n with temperature holds when the wider fitting interval of the magnetic field is used. Thus, we believe that the fall of $1/(eR_H)$ and n evident at $T > 10$ K most likely points to

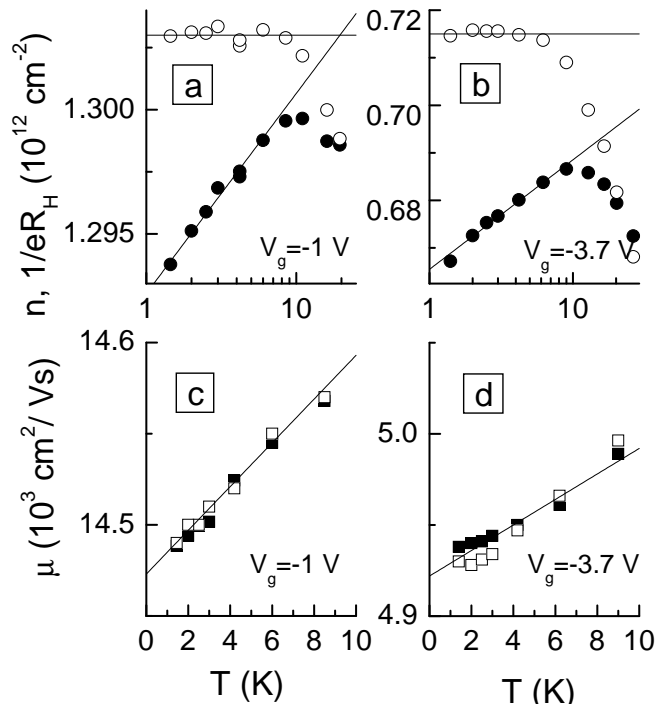


FIG. 2: The temperature dependences of $1/eR_H$ (\bullet), n (\circ) (a, b) and μ (c, d) for structure T1520, measured for $V_g = -1$ V (a, c) and -3.7 V (b, d). Symbols are the experimental data. The values of electron density, n , and mobility μ shown by open symbols have been obtained from the fitting of σ_{xy} -vs- B experimental plots. The solid symbols for μ are obtained from the fit of σ_{xx} -vs- B curves. Lines in (a) and (b) are provided as a guide for the eye. Straight lines in (c) and (d) are drawn through the experimental points and show the extrapolation to $T = 0$.

the fact that the electron density decreases at these temperatures. The possible reason of the decreasing is the transition of some part of electrons from the well to the states of residual donors in the buffer layer, to the states at the heterointerface, to states near the substrate/buffer boundary or near the surface. The decreasing of $1/(eR_H)$ with the temperature increase is observed for all the electron density in both structures investigated. The explicit reason of the downturn of $1/(eR_H)$ remains unknown therefore we restrict our analysis to the low temperature, $T < 9 - 10$ K.

The behavior of the second fitting parameter, which is μ' , is shown in Figs. 2(c) and 2(d). As seen, it increases with the temperature increase for both cases, this increasing is close to the linear one. The physical reason of such behavior will be discussed below.

Now we are in position to consider the role of the e - e interaction. There are different ways to extract experimentally the e - e contribution. They follow from Eqs. (7) and (8) for the conductivity tensor components, and can be outlined as follows: (i) the direct analysis of the magnetic field dependence of σ_{xx} and σ_{xy} ; (ii) the analysis of the parabolic-like negative magnetoresistance [see Eq. (9)

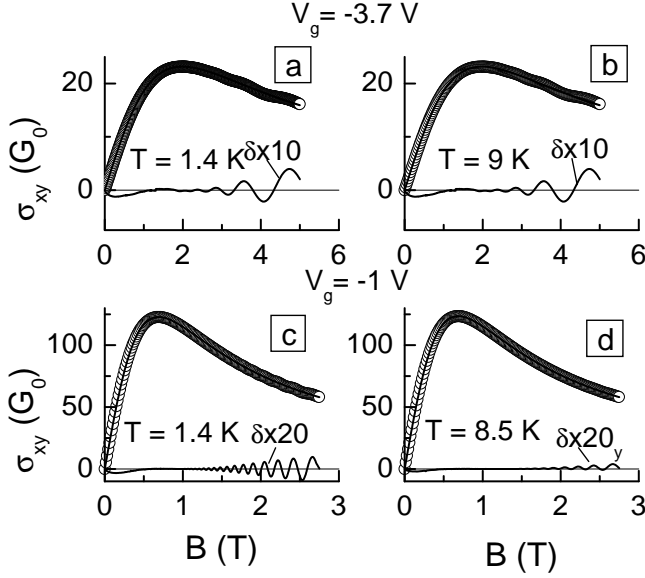


FIG. 3: The magnetic field dependences of σ_{xy} measured for different temperatures for $V_g = -3.7$ V (a,b) and $V_g = -1$ V (c,d), structure T1520. Symbols are the experimental data, solid curves are the fit by Eq. (8) with n and μ' as fitting parameters. Curves labeled as $\delta \times 10$ (a,b) and $\delta \times 20$ (c,d) are the difference between experimental and fitting curves multiplied by a factor 10 or 20, respectively.

below]; (iii) the analysis of the temperature dependencies of σ_{xx} and σ_{xy} in high magnetic field, $B \gg B_{tr}$, when the WL-correction is strongly suppressed; (iv) the analysis of the temperature dependence of the Hall coefficient [see Eq. (10)]; (v) the analysis of the temperature dependence of the conductivity at $B = 0$.

Actually, if one firmly believes that the e - e interaction is the sole mechanism, which determines the temperature and magnetic field dependences of the conductivity, all the methods are not independent and have to duplicate each other. However, if there are any additional mechanisms, for instance, temperature dependent disorder, classical magnetoresistance, *etc.*, the comparison of the results of different methods gives a possibility to estimate the role of “additional” mechanisms and is necessary for elucidating of the contribution of e - e interaction more reliably. Let us apply all listed methods in turn and analyze our experimental results from this point of view.

The first way of the finding of the e - e correction follows from Eqs. (7) and (8). One can fit the experimental σ_{xx} -vs- B curve by Eq. (7) using $\delta\sigma_{xx}^d$ and μ' as the fitting parameters, and n , found from the fit of the experimental σ_{xy} -vs- B curve (see Fig. 2(a,b)). Figures 4(a-d) show the result of the fitting procedure carried out in the magnetic field range from $B = 20 B_{tr}$ to $B = 1.5/\mu$. As seen, an agreement is excellent for all gate voltages and temperatures. The values of the diffusion correction found by this way are presented in Fig. 5(a) as a $\delta\sigma_{xx}^d$ -vs- $T\tau$

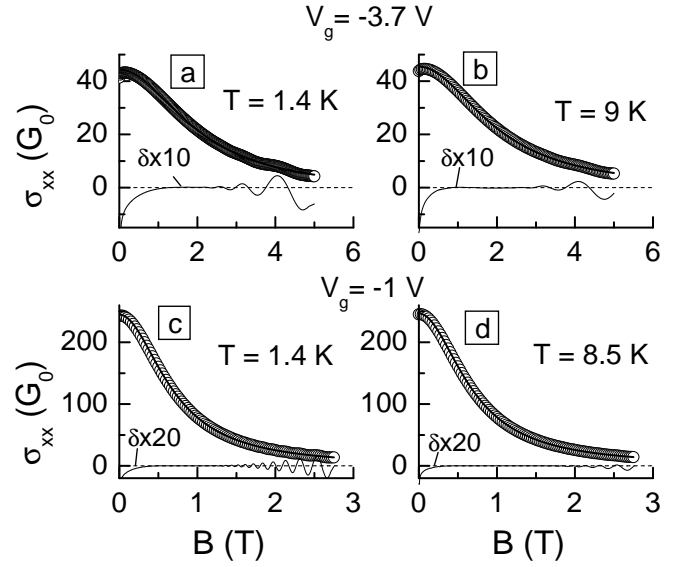


FIG. 4: (a-d) – The magnetic field dependences of σ_{xx} for different temperatures and $V_g = -3.7$ V (a,b) and $V_g = -1$ V (c,d), structure T1520. Symbols are the experimental data, solid curves are the fit by Eq. (7). Curves labeled as $\delta \times 10$ (a,b) and $\delta \times 20$ (c,d) are the difference between experimental and fitting curves multiplied by a factor 10 or 20, respectively.

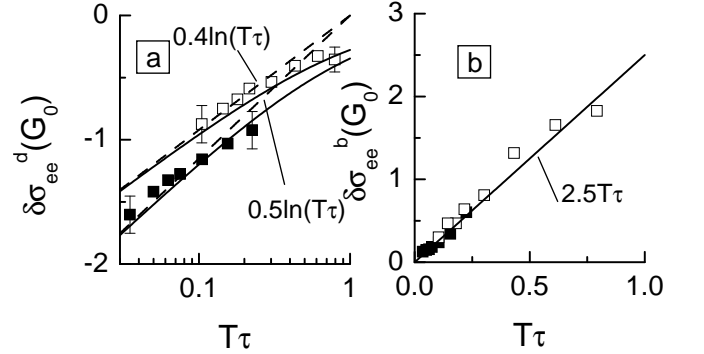


FIG. 5: The temperature dependences of the diffusion (a) and ballistic (b) corrections. Symbols are the experimental data for $V_g = -3.7$ V (■) and -1 V (□). Solid lines in (e) are the improved expression, Eq. (12), for the diffusion correction.

plot. It is seen that the temperature dependence of $\delta\sigma_{xx}^d$ at $T\tau < 0.4$ is close to logarithmic $\delta\sigma_{xx}^d = K_{ee}G_0 \ln(T\tau)$ with $K_{ee} \approx 0.5$ and 0.4 for $V_g = -3.7$ V and -1 V, respectively.

Note, $\delta\sigma_{xx}^d$ is obtained by this way as difference between two large quantities known with some error: the experimental quantity σ_{xx} and the quantity $en\mu'/(1 + \mu'^2 B^2)$ [see Eq. (7)], in which n is also experimental. To estimate this error we have fitted the data within different magnetic field range. The equally good agreement between experimental and calculated curves is observed in all the cases, however the values of $\delta\sigma_{xx}^d$ is somewhat

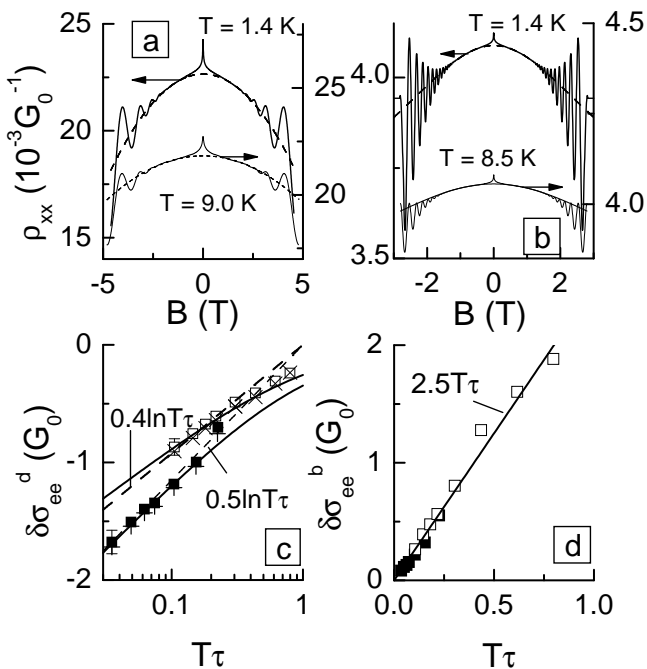


FIG. 6: (a) and (b) – The parabolic-like magnetoresistance for different temperatures for $V_g = -3.7$ V and -1 V, respectively, structure T1520. Solid curves are the experimental data. Dashed curves are the fit by Eq. (9). (c) and (d) – The temperature dependences of the diffusion and ballistic corrections, respectively. Symbols are the experimental data for $V_g = -3.7$ V (\blacksquare , \blackcross) and -1 V (\square , \times) obtained by the second (\blacksquare , \square) and third (\blackcross , \times) ways. Solid lines in (c) are the improved formula for the diffusion $e-e$ correction, Eq. (12).

different (see error bars in Fig. 5(a)).

The value of the second fitting parameter μ' found in this procedure is presented in Figs. 2(b) and 2(d) in which the μ' -values found from the σ_{xy} -vs- B dependence were shown. One can see that the fit of both σ_{xx} and σ_{xy} components gives the μ' -values, which coincide with an accuracy of about (1–2) % and demonstrate close to the linear temperature dependence.

What is the mechanism of the temperature dependence of μ' ? The degeneracy of the electron gas within the actual temperature range, $T < 10$ K, remains strong: $E_F/T > 30$ for $V_g = -3.7$ V and $E_F/T > 55$ for $V_g = -1$ V. Therefore, the ionized impurities or roughness scattering mechanisms cannot lead to a mobility variation with temperature. Obviously, the phonon scattering is also not responsible for such an effect, because it has to lead to the mobility decreasing with the temperature increase, which is opposite to that observed experimentally for μ' . So, we believe that the temperature dependence of μ' results from the ballistic part of the electron-electron interaction, which in the main really reduces to renormalization of the mobility as we supposed writing Eqs. (7) and (8) out. The temperature dependence of the ballistic part defined as $\delta\sigma_{ee}^b(T) = en\delta\mu(T)$ with $\delta\mu(T) = \mu'(T) - \mu'(0)$ is presented in Fig. 5(b). One

can see that $\delta\sigma_{ee}^b$ linearly increases with temperature and all the experimental points lie on the same straight line $\delta\sigma_{ee}^b(T)/G_0 \simeq 2.5T\tau$ for both gate voltages. It is important for the following to note that the variation of $\delta\sigma_{ee}^b$ in our temperature range is larger for $V_g = -1$ V than that for the case of $V_g = -3.7$ V. It is sequence of the higher value of the transport relaxation time τ in the first case (see Table I).

It should be mentioned, that the discrepancy between the experimental σ_{xx} -vs- B curves and calculated ones at low magnetic field, resulting from the WL correction, continues up to high magnetic field, $(15 - 20) B_{tr}$ [see Figs. 4(a)– 4(d)]. Therefore, if one uses the range of the magnetic field including the lower fields in the fitting procedure, we can obtain the wrong value of the correction.

The second way is based on the analysis of the parabolic-like negative magnetoresistance. It directly follows from Eqs. (7) and (8) that the magnetoresistance should have the form

$$\rho_{xx}(B, T) \simeq \frac{1}{en\mu'} - \frac{1}{(en\mu')^2} (1 - \mu'^2 B^2) \delta\sigma_{xx}^d(T). \quad (9)$$

Thus, fitting the experimental ρ_{xx} -versus- B curve for a given temperature by Eq. (9) one can find both the diffusion and ballistic corrections. This method is free of disadvantage of the previous one because $\delta\sigma_{xx}^d$ is obtained not as a difference between two large values. As Figs. 6(a) and 6(b) show Eq. (9) excellently describes the experimental data. The temperature dependence of $\delta\sigma_{ee}^d$ and $\delta\sigma_{ee}^b$ found from the fit are presented in Figs. 6(c) and 6(d). Comparison with the results presented in Figs. 5(a) and 5(b) shows a good agreement with the data obtained by the first way.

The third way is the analysis of the temperature dependence of the Hall coefficient, $R_H = \sigma_{xy}/[B(\sigma_{xy}^2 + \sigma_{xx}^2)]$. It follows from Eqs.(7) and (8) that the diffusion interaction correction should be equal to

$$\delta\sigma_{xx}^d(T) = \frac{[R_H(T) - (en)^{-1}]en\mu'}{2R_H(T)}. \quad (10)$$

To find $\delta\sigma_{xx}^d(T)$, we use the values of n and μ' obtained from analysis of σ_{xy} -versus- B dependences and the temperature dependence of R_H [see Figs. 2(a) and 2(b)]. The results of such data processing are plotted in Fig. 6(c) by crosses. One can see that the value of the interaction correction and its temperature dependence are very close to ones obtained with the use of the previous methods. It should be stressed that the analysis of the Hall coefficient gives the diffusion correction only.

The fourth way is the analysis of the temperature dependence of σ_{xx} at high enough magnetic field where WL is suppressed. For strictly diffusion regime the σ_{xx} -component should logarithmically depend on the temperature while σ_{xy} should be temperature independent [see Eqs. (4) and (5)]. In Fig. 7 we have plotted the variation of σ_{xx} and σ_{xy} with the temperature at different magnetic fields (reference temperature is $T = 1.4$ K). It is

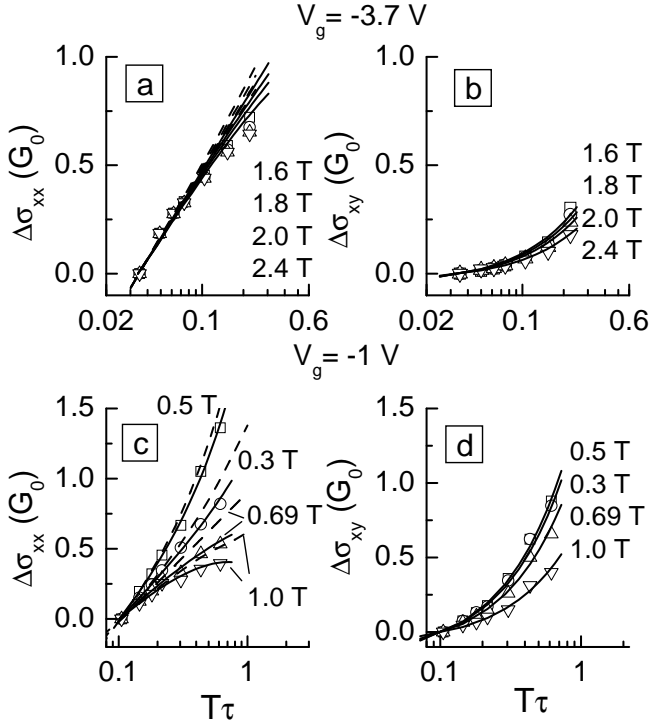


FIG. 7: The temperature dependence of $\Delta\sigma_{xx}$ (a,c) and $\Delta\sigma_{xy}$ (b,d) for different magnetic fields in vicinity of $B = 1/\mu$ for $V_g = -3.7$ V (a,b) and $V_g = -1$ V (c,d). Symbols are the experimental results for $B = 1.6$ (\square), 1.8 (\circ), 2.0 (\triangle), and 2.4 T (∇) (a,b), and $B = 0.3$ (\square), 0.5 (\circ), 0.69 (\triangle), and 1.0 T (∇) (c,d). Dashed lines are Eqs. (7) and (8) with $\mu'(T)$ presented in Figs. 2(b) and 2(d) and $\delta\sigma_{xx}^d(T)$ given by Eq. (6) with $K_{ee} = 0.45$ and 0.4 for $V_g = -3.7$ V and -1 V, respectively. Solid lines are obtained analogously, but $\delta\sigma_{xx}^d(T)$ is calculated from the improved formula, Eq. (12). Solid lines in panels (b) and (d) coincide with dashed ones because $\delta\sigma_{xx}^d(T)$ does not contribute to σ_{xy} .

clearly seen that $\Delta\sigma_{xx}$ for $V_g = -3.7$ V does not practically depend on the magnetic field. At $T\tau \lesssim 0.1$ the temperature dependence of $\Delta\sigma_{xx}$ is logarithmic. The slope is approximately equal to 0.45 that is very close to that obtained with the help of above methods. The temperature dependence of $\Delta\sigma_{xy}$ is significantly weaker and, as will be shown below, results from the ballistic contribution via the mobility renormalization.

The significantly different behavior is demonstrated by the data obtained at $V_g = -1$ V. First of all, both the $\Delta\sigma_{xx}$ -vs- T and $\Delta\sigma_{xy}$ -vs- T plots taken at different B represent fan charts. Second, the variation of σ_{xy} with the temperature is comparable in magnitude with that for σ_{xx} . Obviously, both facts are a sequence of the temperature dependence of the ballistic contribution, which is larger in magnitude for this gate voltage due to higher value of $T\tau$. Nevertheless, the diffusion contribution can be easily extracted in this case as well. In framework of the model used, which reduces the ballistics to mobility renormalization, the ballistic correction to σ_{xx} is equal to

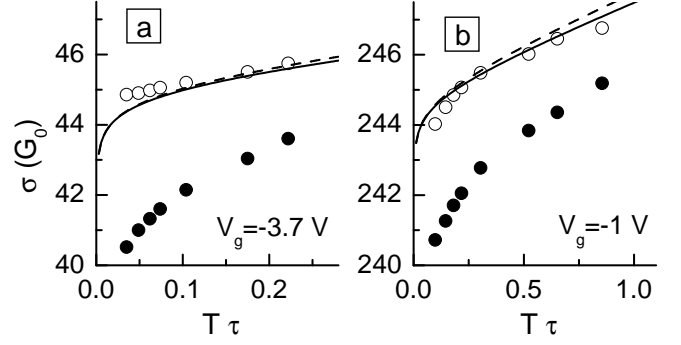


FIG. 8: The temperature dependences of the conductivity at $B = 0$. Solid symbols are for the conductivity measured experimentally. Open symbols are the same data after subtraction of the interference quantum correction. Lines are drawn as described in the text.

zero when $\mu B = 1$. Really, differentiating Eq. (7) with respect to μ one obtains:

$$\delta\sigma_{xx}^b = \frac{\partial\sigma_{xx}}{\partial\mu}\delta\mu = \frac{1 - \mu^2 B^2}{(1 + \mu^2 B^2)^2} en \delta\mu \Big|_{\mu B=1} = 0. \quad (11)$$

That is why the temperature dependence of σ_{xx} at $B = 1/\mu$ should be wholly determined by the diffusion correction. Inspection of Fig. 7(c) shows that the temperature dependence of σ_{xx} at $B = 1/\mu = 0.69$ T is actually close to logarithmic up to $T\tau \simeq 0.25$ with the slope 0.4 , which coincides with that found before [see Figs. 5(a) and 6(c)].

Let us inspect how the model used describes the temperature dependences of $\Delta\sigma_{xx}$ and $\Delta\sigma_{xy}$ at $\mu B \neq 1$. In Fig. 7 we plot the curves calculated from Eqs. (7) and (8) with $\mu'(T)$ presented in Figs. 2(b) and 2(d), and $\delta\sigma_{xx}^d(T)$ given by Eq. (6) with $K_{ee} = 0.45$ and 0.4 for $V_g = -3.7$ V and -1 V, respectively. One can see that our model perfectly describes the data for $\Delta\sigma_{xy}$ [see Figs. 7(b) and 7(d)]. As for the temperature dependence of $\Delta\sigma_{xx}$, there is satisfactory agreement between the data and calculated results up to $T\tau \simeq 0.3$ [dashed lines in Figs. 7(a) and 7(c)]. At higher $T\tau$ values a discrepancy between calculated curves is evident, the stronger magnetic field the more pronounced discrepancy is. In the next section we propose an improvement of Eq. (6) for the diffusion contribution, which gives an excellent accordance over the whole $T\tau$ -range.

Up to now we determined the interaction correction in the presence of a magnetic field. Let us now turn to the last method and consider the correction at $B = 0$. The experimental temperature dependences of the conductivity at $B = 0$ are presented in Fig. 8 by solid circles. Since this dependence is determined by both the WL and interaction correction, one should exclude the WL contribution to find the interaction contribution. For this purpose we have measured the low-field magnetoresistance [Figs. 9(a) and 9(b)] caused by suppression of the WL correction. Analyzing the shape of magnetoresistance

curves using standard procedure^{18,19} we have found the phase relaxation time (τ_ϕ) and its temperature dependence [Fig. 9(c)]. After that the WL quantum correction has been calculated according to Eq. (2) and subtracted from the experimental values of conductivity at $B = 0$. Thus, we have obtained the conductivity, which temperature dependence is caused only by the interaction corrections [shown by open symbols in Figs. 8(a) and 8(b)]. To compare these data with the results obtained above, we have calculated T -dependences of $en\mu(0) + \delta\sigma_{ee}^d + \delta\sigma_{ee}^b$ using $\mu(0)$ from Table I, $\delta\sigma_{ee}^b = 2.5 G_0 T\tau$, and $\delta\sigma_{ee}^d(T) = 0.45 G_0 \ln(T\tau)$ and $0.4 G_0 \ln(T\tau)$ for $V_g = -3.7$ V and -1 V, respectively. The results are shown in Fig. 8 by dashed lines. So, the parameters obtained in the presence of magnetic field well describe the temperature dependence of the conductivity at zero magnetic field.

Thus, we have found the diffusion and ballistic contributions of the interaction correction to the conductivity by the different ways. The fact that all these methods give close results shows that other “parasitic” mechanisms, which could contribute to the temperature and magnetic field dependences, are negligible. We turn now to discussion.

IV. DISCUSSION

First of all, let us consider the absolute value of the diffusion part of the interaction correction. As noted in Section II the authors of Ref. 1 “have chosen the

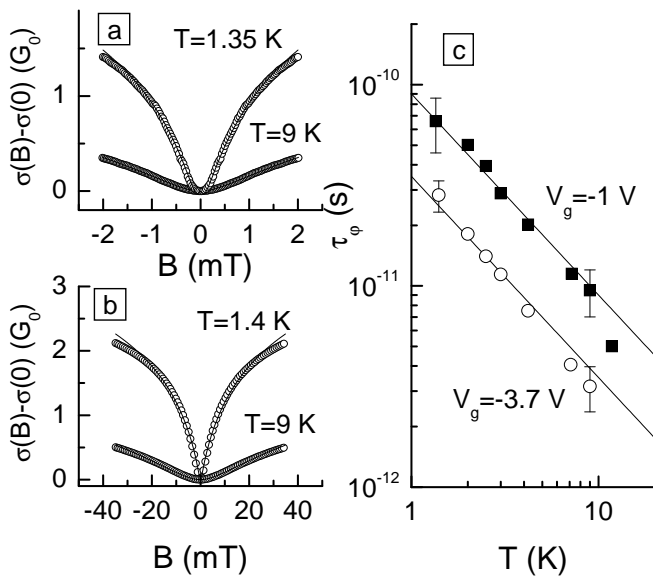


FIG. 9: (a, b) – The magnetoconductivity caused by suppression of the interference quantum correction measured at two temperatures and two gate voltages. Symbols are the experimental data. Curves are the best fit by formulae from Ref. 18,19 with τ_ϕ presented for different temperatures in panel (c). Lines in (c) are T^{-1} -law.

argument of the logarithm in Eq. (3) to be E_F/T instead of the usual $1/T\tau$ to emphasize that contrary to the naive expectations the logarithmic term persists up to temperatures much larger than $1/\tau$. It means that the logarithmic part of the correction can be written as $-K_{ee}G_0[\ln(k_{Fl}/2) - \ln(T\tau)]$. The question is: does temperature independent term $-K_{ee}G_0 \ln(k_{Fl}/2)$ contribute to $\delta\sigma_{xx}^d$ or not? To clarify we have plotted in Fig. 10 the both theoretical $T\tau$ -dependences [Eq. (6) and logarithmic part of Eq. (3)], using K_{ee} found from the temperature dependence of σ_{xx} (forth method) and parameters from Table I. In the same figure we present the experimental data for $V_g = -1$ V when the Drude conductivity is maximal in magnitude. Mere it is not needed to involve the $-K_{ee}G_0 \ln(k_{Fl}/2)$ -term to describe the experiment. Any temperature independent contribution that might exist in σ_{xx}^d is lower than $(0.1 - 0.2)G_0$.

Thus, two parts of the logarithmic correction are different. In the presence of a magnetic field, the first one, $K_{ee}G_0 \ln(T\tau)$, contributes only to σ_{xx} but does not to σ_{xy} . Just this term we figure out experimentally. The second term, $-K_{ee}G_0 \ln(k_{Fl}/2)$, contributes both to σ_{xx} and to σ_{xy} and, in fact, reduces to the renormalization of the transport relaxation time, i.e., the mobility.

Next issue, which should be pointed out is the parabolic-like negative magnetoresistance in the high magnetic field. Fig. 6(a,b) shows that at low $T\tau$ value such a behavior is observed against a background of the Shubnikov-de Haas oscillations far exceeding the magnetic field $B = 1/\mu$. However, at large $T\tau$ -value the monotonic part of the experimental curve runs noticeably steeper at $B \gtrsim 2/\mu$ [see lower curves in Fig. 6(b)]. From our point of view, it can be resulted from the $e-e$ interaction as well. As shown in Ref. 3 in presence of long-range potential the ballistic contribution is suppressed at $B = 0$ and restores at high magnetic field. Because in our structures the ballistic correction is positive, it is equivalent to the mobility increase that, in its turn, leads to additional decreasing of ρ_{xx} with B -increase at $B > 1/\mu$. This effect is proportional to the ballistic contribution and therefore reveals itself at $V_g = -1$ V when the value of $T\tau$ is larger. The analogous deviation of ρ_{xx} from parabola was observed in Ref. 5. The interpretation was also based on the magnetic field dependence of the ballistic part of the $e-e$ interaction correction.

Let us finally discuss the diffusion correction at large $T\tau$. As seen from Figs. 5(a), 6(c) at $T\tau \lesssim 0.2 - 0.3$ its temperature dependence is close to the logarithmic one. However at larger $T\tau$ the systematic deviation down is evident. Besides, the temperature dependence of σ_{xx} at $T\tau > 0.2 - 0.3$ for different B is described in the framework of the model used only qualitatively [see Fig. 7(a,c)]. We have found that the agreement can be improved if one replaces the argument $1/(T\tau)$ in logarithm in Eq. (6) by $1/(T\tau) + 1$ that removes the divergence of diffusion contribution with $T\tau$ -increase:

$$\frac{\delta\sigma_{xx}^d(T)}{G_0} = - \left[1 + 3 \left(1 - \frac{\ln(1 + F_0^\sigma)}{F_0^\sigma} \right) \right] \ln \left(\frac{1}{T\tau} + 1 \right)$$

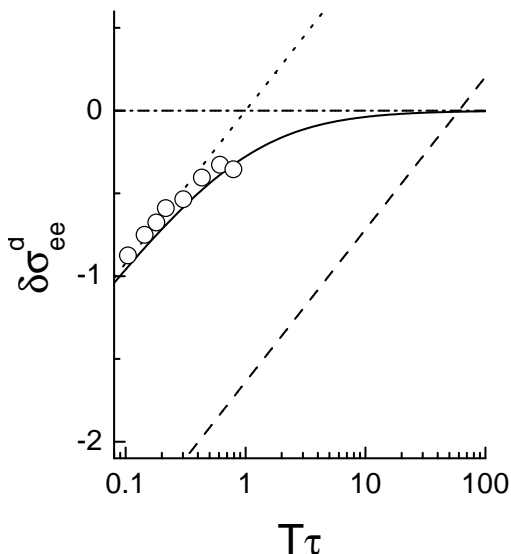


FIG. 10: The $T\tau$ -dependence of $\delta\sigma_{ee}^d$ for $V_g = -1$ V. Symbols are the experimental results. Dotted and dashed lines are dependences $K_{ee} G_0 \ln T\tau$ and $K_{ee} G_0 [\ln T\tau - \ln(k_{Fl}/2)]$, respectively. Solid line is the dependence $-K_{ee} G_0 \ln [1/(T\tau) + 1]$, Eq. (12). In all the cases $K_{ee} = 0.4$.

$$\equiv -K_{ee} \ln \left(\frac{1}{T\tau} + 1 \right), \quad (12)$$

After such modification the agreement with the experimental data becomes excellent within whole $T\tau$ range as Figs. 5(a), 6(c), 7, and 8 demonstrate. It should be mentioned that Eq. (12) in combination with Eqs. (7) and (8) reproduces the $1/T$ temperature dependence of ballistic asymptotics of $\delta\rho_{xx}(T)/B^2$ and $\delta R_H(T)/B$, in a qualitative agreement with Refs. 3 and 10, respectively. The numerical coefficients in front of these asymptotics depend on details of disorder and were calculated in Refs. 3 and 10 only for the case of a purely white-noise disorder and thus should not be necessarily reproduced in experiments on realistic structures.

Analogous measurements were performed for the structure 3510, where the electron density and mobility were controlled by illumination due to persistent photoconductivity (see Table I). The parameter $T\tau$ for this structure laid within the interval from 0.07 to 0.7. All five ways of determination of the interaction correction described above give consistent results also. It turns out that the values and the temperature dependences both of the diffusion and ballistic corrections are very close to that for structure T1520.

In the framework of theory¹ the interaction corrections are governed by the Fermi-liquid parameter F_0^σ for the diffusion correction and by \tilde{F}_0^σ for the ballistic one [see Eq. (3)], these parameters depend on r_s only. The values of F_0^σ and \tilde{F}_0^σ obtained for both structures investigated in this paper and F_0^σ found in our previous papers^{20,21} are shown in Fig. 11.²⁵ One can see that all the data correlate well. The r_s -dependences of both F_0^σ and \tilde{F}_0^σ are close to

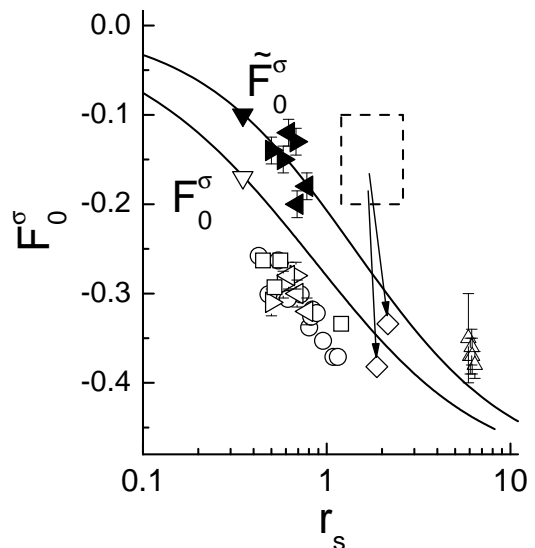


FIG. 11: The r_s -dependence of the Fermi-liquid constants F_0^σ and \tilde{F}_0^σ . Lines are calculated according to Ref. 1. Symbols are the experimental results for structures T1520 ($\blacktriangleright, \triangleright$) and 3510 ($\blacktriangleleft, \triangleleft$), for the samples with $k_{Fl} > 5$ from Ref. 20 (\circ), structures from Ref. 21 (\square), Ref. 23 (\triangle), and Ref. 22 ($\nabla, \blacktriangledown$). Dashed box indicates an approximate range of r_s and F_0^σ for the structures from Ref. 5,7. (\diamond) – The new F_0^σ values for two samples from Ref. 5 obtained in our interpretation (see the text for details). Open and solid symbols are for F_0^σ and \tilde{F}_0^σ , respectively.

theoretical ones, though the experimental points for F_0^σ fall systematically below the corresponding theoretical curve.

Let us compare our results with that obtained by other authors for the analogous 2D electron systems. Recently, the paper by Renard *et al.*²² devoted to an experimental study of very-low-mobility GaAs quantum wells in a temperature range 1.5 – 110 K has been released. The value of the parameter $T\tau$ in these systems was less than 0.3 even at the highest temperature. So, only the beginning of the crossover from the diffusive to the ballistic regime is spanned in this paper. The gas parameter r_s in samples investigated was equal to 0.3 – 0.35. The authors were able to describe the longitudinal conductivity and the Hall effect within framework of the theories^{1,10} using the theoretical values of F_0^σ and \tilde{F}_0^σ from Ref. 1 (shown by ∇ and \blacktriangledown in Fig. 11). Some difference in the interpretation of the data in Ref. 22 with respect to our analysis is result of the fact that the range of the magnetic field in this paper was limited by the value of about $8 B_{tr}$. Figs. 4(a–d) show that the interference correction under this condition is not completely suppressed. We suppose that neglect of this fact gives some error in determination of the value of the e - e correction.

The e - e interaction correction in GaAs 2D systems of high quality with extremely low electron density was systematically studied in Ref. 23. It has been shown that the theory¹ consistently describes the temperature de-

pendences of the conductivity in zero-magnetic field and of the Hall resistivity in different magnetic fields. The parameters F_0^σ extracted from $\sigma(T)$ and $\rho_{xy}(T)$ are close to each other. As seen from Fig. 11 the data from this paper shown by open triangles correlate well with our results despite the large r_s value.

The role of this correction within wide $T\tau$ range was studied also in the papers by Galaktionov *et al.*⁷ and Li *et al.*⁵ They investigated GaAs heterostructures with the relatively high electron mobility at $T\tau \simeq 0.03 - 0.3$. The authors presumed that the scattering was governed by the long-range potential and therefore applied the theory by Gornyi and Mirlin.^{2,3} The values of the Fermi-liquid parameter obtained in this paper (indicated in Fig. 11 by dashed box) strongly differ from our and all other results. It should be noted that the authors restricted themselves by consideration of $\rho_{xx}(B)$ and has not analyzed other effects. If one reinterprets these data supposing that the white-noise disorder is the main scattering potential, the parabolic-like negative magnetoresistance within the framework of our model should be determined by the diffusion correction only. Retreating the data presented in Fig. 1 from Ref. 5 for two samples with $n = 6.8 \times 10^{10}$ and $9 \times 10^{10} \text{ cm}^{-2}$ in such a manner, we obtain the new values of F_0^σ (diamonds in Fig. 11), which accord well with the other results.

V. CONCLUSION

We have experimentally studied the electron-electron interaction correction to the conductivity of two-dimensional electron gas in $\text{Al}_x\text{Ga}_{1-x}\text{As}/\text{GaAs}/\text{Al}_x\text{Ga}_{1-x}\text{As}$ and GaAs/In_x

$\text{Ga}_{1-x}\text{As}/\text{GaAs}$ single-quantum-well heterostructures in a wide range of $T\tau$ -parameter, $T\tau = 0.03 - 0.8$, covering the diffusion and ballistic regimes. We have shown that the correction is separated into two parts, which are distinguished by the manner how they modify the conductivity tensor in the presence of a magnetic field. The first part, or the diffusion correction, contributes to σ_{xx} only. The contribution to σ_{xy} is equal zero. The experimental value and the temperature dependence of the diffusion correction is proportional to $\ln[1/(T\tau) + 1]$, Eq. (12). We have shown that this part does not include the temperature independent term $-K_{ee}G_0 \ln(E_F\tau)$. The second part of the interaction correction, the ballistic part, is reduced to the renormalization of the transport relaxation time τ , that results in appearance of the temperature dependence of the mobility. The ballistic correction linearly increases with the temperature increase. This model allows us to describe consistently the behavior of the components both of the resistivity and of the conductivity tensors with magnetic field and temperature as well as the temperature dependence of the conductivity without magnetic field. We have experimentally determined the values of the Fermi-liquid parameters F_0^σ and \tilde{F}_0^σ and found them to be close to those predicted theoretically.

Acknowledgments

We thank Igor Gornyi for useful discussion. This work was supported in part by the RFBR (Grants 03-02-16150, 04-02-16626, and 05-02-16413), the CRDF (Grants EK-005-X1 and Y1-P-05-11), and the INTAS (Grant 1B290).

-
- ¹ G. Zala, B. N. Narozhny, and I. L. Aleiner, Phys. Rev. B **64**, 214204 (2001).
² I. V. Gornyi and A. D. Mirlin, Phys. Rev. Lett. **90**, 076801 (2003).
³ I. V. Gornyi and A. D. Mirlin, Phys. Rev. B **69**, 045313 (2004).
⁴ V. M. Pudalov, M. E. Gershenson, H. Kojima, G. Brunthaler, A. Prinz, and G. Bauer, Phys. Rev. Lett **91**, 126403 (2003).
⁵ L. Li, Y. Y. Proskuryakov, A. K. Savchenko, E. H. Linfield, and D. A. Ritchie, Phys. Rev. Lett **90**, 076802 (2003).
⁶ Y. Y. Proskuryakov, A. K. Savchenko, S. S. Safonov, M. Pepper, M. Y. Simmons, and D. A. Ritchie, Phys. Rev. Lett **89**, 076406 (2002).
⁷ E. A. Galaktionov, A. K. Savchenko, S. S. Safonov, Y. Y. Proskuryakov, L. Li, M. Pepper, M. Y. Simmons, D. A. Ritchie, E. H. Linfield, and Z. D. Kvon, in *Fundamental Problems of Mesoscopic Physics: Interactions and Decoherence*, edited by I. V. Lerner, B. L. Altshuler, and Y. Gefen (Kluwer Academic Publishers, Dordrecht, 2004), p. 349; cond-mat/0402139 (unpublished).
⁸ B. L. Altshuler, D. L. Maslov, and V. M. Pudalov, Physica

- E **9**, 209 (2001).
⁹ A. Dmitriev, M. Dyakonov, and R. Jullien, Phys. Rev. B **64**, 233321 (2001).
¹⁰ G. Zala, B. N. Narozhny, and I. L. Aleiner, Phys. Rev. B **64**, 201201 (2001).
¹¹ A. P. Dmitriev, V. Y. Kachorovskii, and I. V. Gornyi, Phys. Rev. B **56**, 9910 (1997).
¹² B. L. Altshuler and A. G. Aronov, in *Electron-Electron Interaction in Disordered Systems*, Edited by A. L. Efros and M. Pollak (North Holland, Amsterdam, 1985).
¹³ A. M. Finkelstein, Zh. Éksp. Teor. Fiz. **84**, 168 (1983) [Sov. Phys. JETP **57**, 97 (1983)]; Z. Phys. B: Condens. Matter **56**, 189 (1984).
¹⁴ C. Castellani, C. Di Castro, P. A. Lee, and M. Ma, Phys. Rev. B **30**, 527 (1984); **30**, 1596 (1984); C. Castellani, C. Di Castro, and P. A. Lee, *ibid.* **57**, 9381(R) (1998).
¹⁵ G. M. Minkov, A. A. Sherstobitov, A. V. Germanenko, O. E. Rut, V. A. Larionova, and B. N. Zvonkov, Phys. Rev. B **71**, 165312 (2005).
¹⁶ D. A. Poole, M. Pepper, and R. W. Glew, J. Phys C: Solid State Phys **14**, L995 (1981).
¹⁷ D. J. Newson, M. Pepper, E. Y. Hall, and G. Hill, J. Phys.

- C: Solid State Phys **20**, 4369 (1987).
- ¹⁸ S. Hikami, A. I. Larkin, and Y. Nagaoka, Prog. Theor. Phys. **63**, 707 (1980).
- ¹⁹ H.-P. Wittmann and A. Schmid, J. Low Temp. Phys. **69**, 131 (1987).
- ²⁰ G. M. Minkov, O. E. Rut, A. V. Germanenko, A. A. Sherstobitov, V. I. Shashkin, O. I. Khrykin, and B. N. Zvonkov, Phys. Rev. B **67**, 205306 (2003).
- ²¹ G. M. Minkov, O. E. Rut, A. V. Germanenko, A. A. Sherstobitov, V. I. Shashkin, O. I. Khrykin, and V. M. Daniltsev, Phys. Rev. B **64**, 235327 (2001).
- ²² V. T. Renard, I. V. Gornyi, O. A. Tkachenko, V. A. Tkachenko, Z. D. Kvon, E. B. Olshanetsky, A. I. Toropov, and J.-C. Portal, Phys. Rev. B **72**, 075313 (2005).
- ²³ C. E. Yasin, T. L. Sobey, A. P. Micolich, A. R. Hamilton, M. Y. Simmons, L. N. Pfeiffer, K. W. West, E. H. Linfield, M. Pepper, and D. A. Ritchie, cond-mat/0403411 (unpublished).
- ²⁴ The detailed studies of the low field behavior of ρ_{xy} reveals some nonlinearity of the ρ_{xy} -vs- B dependence at $B < (2 - 3)B_{tr}$. Just in this magnetic field range the WL correction determines the magnetic field dependence of ρ_{xx} . Such a behavior was already reported in Ref. 16,17 and, we believe, exists in the most of the 2D structures. Probably, experimentalists do not like to publish the results of such a kind, because the theory does not predict the magnetic field dependence of the Hall coefficient due to the weak localization.
- ²⁵ As shown in Ref. 20, the experimental value of F_0^σ depends not only on the gas parameter r_s , as it should be theoretically in the case of $k_F l \gg 1$, but on the disorder strength as well. Therefore, in Fig. 11 we present the data from Ref. 20 relating to the relatively high value of $k_F l$: $k_F l > 5$.